X-625-74-50
PREPRINT

ION COMPOSITION AND DRIFT OBSERVATIONS IN THE NIGHTTIME EQUATORIAL IONOSPHERE

R. A. GOLDBERG
A. C. AIKIN
B. V. KRISHNA MURTHY

FEBRUARY 1974

GODDARD SPACE FLIGHT CENTER
GREENBELT, MARYLAND

ION COMPOSITION AND DRIFT OBSERVATIONS IN THE NIGHTTIME EQUATORIAL IONOSPHERE

by

R. A. Goldberg
A. C. Aikin
Laboratory for Planetary Atmospheres
NASA Goddard Space Flight Center
Greenbelt, Maryland

and

B. V. Krishna Murthy
Space Science and Technology Center
Trivandrum, India

ABSTRACT

The first in situ measurements of ion composition in the nighttime equatorial E and F region ionospheres (90-300 km) are presented and discussed. These profiles were obtained by two rocket-borne ion mass spectrometers launched from Thumba, India on March 9-10, 1970 at solar zenith angles of 112° and 165°. Ionosonde data established that the composition was measured at times bounding a period of F region downward drift. During this period the ions O^+ and N^+ were enhanced by one to three orders of magnitude between 220 and 300 km. Below the drift region (200 km), O^+ ceased to be the major ionic constituent but the concentrations of O^+ and N^+ remained larger than predicted from known radiation sources and loss processes. Here also, both the O_2^+ and NO^+ profiles retained nearly the same shape and magnitude throughout the night in agreement with theories assuming scattered UV radiation to be the maintaining source. Light metallic ions including Mg^+, Na^+ and possibly Si^+ were observed to altitudes approaching 300 km, while the heavier ions Ca^+ and K^+ were seen in reduced quantity to 200 km. All metal ion profiles exhibited changes which can be ascribed to vertical drifting.

INTRODUCTION

At the magnetic equator the F region exhibits a vertical drift which is correlated with E region dynamo electric fields. Rocket studies of electron density (Aikin and Blumle, 1968) and incoherent backscatter soundings (Farley, 1966; Balsley, 1973) have demonstrated that at night the equatorial F region moves downward enhancing lower F region ionospheric concentrations to values larger than those predicted on the basis of maintenance by scattered solar ultraviolet radiations. A detailed description of the behavior of the nighttime equatorial ionosphere has not been possible because information on temporal changes of nighttime ion composition at lower altitudes has not previously been available.

In this paper we report the first measurements of nighttime equatorial positive ion composition from 90 to 300 km altitude. These profiles were obtained during the night of March 9-10, 1979 with ion mass spectrometers launched from the Indian Thumba Equatorial Rocket Launch Site (TERLS), located at 8.53°N latitude, 76.95°E longitude, and -1.7° magnetic dip (calculated from Stassinopoulos and Mead, 1972). The first launching, rocket 18.97, occurred at a solar zenith angle of 112° (1938 LMT) and the rocket reached an apogee of 298 km. At this time, the F2 peak was near its maximum height, which was in excess of 500 km. Rocket 18.98 was launched at χ = 165° (0108 LMT) and reached 295 km, subsequent to the downward drift of the F region peak to an altitude of approximately 300 km. Transport of the F region during this period was determined from analysis of ionograms taken at frequent intervals.

A third rocket (18.99) launched 35 minutes after 18.98, carried instrumentation to measure ultraviolet radiations important for the

maintenance of the nighttime ionosphere. The details and results of these experiments are discussed by Faresce et al. (1973a, 1973b) and used in the interpretation of the ion composition data.

INSTRUMENTATION AND ANALYSIS

Characteristics of the flights of 18.97 and 18.98 are listed in Aikin and Goldberg (1973). Trajectories were determined using a tone range/telemetry interferometer tracking system (Hudgins and Lease, 1967). Magnetometers were used to provide payload axis-magnetic field angles of 88° (18.97) and 87° (18.98). Payload aspects for both flights were then determined by assuming the payload axis to lie in the trajectory plane.

Each payload underwent nose cone ejection and separation from the rocket motor prior to ion composition sampling. The ion composition was measured using pumped, quadrupole ion mass spectrometers of the type discussed in Goldberg and Aikin (1971). The characteristics of each spectrometer are tabulated in Table I. In addition to ion sampling, total electron density was measured on each flight by means of the continuous wave dispersive Doppler technique (Seddon, 1953; Bauer and Jackson, 1962) operating at transmitting frequencies of 73.60 and 24.53 MHz. Quasi-longitudinal propagation conditions were preserved at the magnetic equator by launching in a southward direction.

Sample mass spectra and the method of data analysis for these rockets are given in Aikin and Goldberg (1973). The total ion spectrometer current for each mass spectrum was normalized to the total electron density at the mean height for the spectrum using the electron density profile obtained by the propagation experiment. Corrections for relative mass effects were applied from free molecular flow theory as discussed in Goldberg and

Blumle (1970). The temperature profiles used to make these corrections were deduced from the U.S. Standard Atmosphere, 1966 Supplement.

Above 200 km and only on the flight of 18.98, a significant background current was superimposed on the spectra. It increased three orders of magnitude by apogee, masking the minor constituents in the upper domains of the flight. This background can be caused by soft energetic electrons in the 2 to 15 Kev energy range, with fluxes similar to those deduced by Heikkila (1971) at higher altitudes. The detailed nature of this background source is discussed elsewhere (Goldberg, 1973); it suffices here to state that the background currents were subtracted from the ion spectral currents to arrive at values used for normalization.

Drift data were obtained from ionogram studies. The ionogram true height analysis was optimized by matching the low end of the ionogram trace to the CW Doppler profile from 18.98. This fit and resulting low density slope was then assumed in the analysis of the ionograms. Direct comparison of the electron density profiles obtained by the two independent techniques showed good agreement.

It should be noted that the night of March 9-10, 1970 occurred after the great magnetic storm of March 8. On the night of March 9-10, the K_p index fluctuated between 4 and 6 indicating a period of moderate activity. Chandra and Rastogi (1972) have shown an inverse correlation between range blanketing spread F and K_p index at the magnetic equator under nighttime conditions. Hence, the moderate magnetic activity of March 9-10, 1970 is consistent with the partial obscuration of the F region ionogram traces observed, and permitted true height analysis from the ionograms for that night.

RESULTS AND DISCUSSION

The curves labelled N_i in Figures 1 and 2 were obtained from the CW propagation electron density experiment aboard each rocket. Other profiles illustrate and compare the time behavior of the non-metallic and metallic ions, respectively. Minor isotopic ions and contaminents, e.g., H_2O^+, were observed but are not shown in the figures. The most noticeable feature seen is the effect of downward transport of atomic ions and electrons, which can be interpreted in terms of the velocity-time plot shown in Figure 3.

The upper portion of Figure 3 illustrates the altitude variations at two constant densities, one near the minimum ($N_e = 5 \times 10^4$ cm^{-3}) and one near the maximum ($N_e = 4 \times 10^5$ cm^{-3}) value for the F2 layer. We note that both portions of the layer moved downward at the same rate implying a preservation of the layer shape during this motion. This supports the suggestion that layer motion approximates drift motion at the nighttime equator, as proposed by Balsley (1969). The slope of the curve depicts the change of isopleth altitude with time and can be used to derive the vertical velocity profile shown below. The launch sequence of the rockets, also indicated in Figure 3, shows the first measurement to have occurred at a time when the altitude of the F2 peak was near 550 km and undergoing an upward drift. The second measurement occurred after the F2 layer peak height had dropped to 300 km altitude and the downward drift had become negligible.

The first measurement was made during a period of upward drift. Following this the F layer moved down, increasing the O^+ concentration at 300 km by nearly three orders of magnitude (cf. Figure 1). Below 200 km

the O^+ concentration decreased between the two measurements, but less rapidly than would be expected from the known nighttime production and loss processes.

There is a measurable concentration of N^+ observed although the altitude distribution differs between the two flights. The earlier flight exhibits a nearly altitude independent distribution of about 20 ions/cm^3. During the flight of 18.98, N^+ assumed a distribution that increased near apogee but decreased below 240 km with respect to the 18.97 distribution. The 18.98 altitude variation of N^+ paralleled that of O^+ but with a reduced abundance.

While drift effects control the number and species distribution of ions above 200 km, drift could not be expected to be important below 200 km, where the time constant for the loss of both O^+ and N^+ is very short and the major ions observed are molecular, i.e., NO^+ and O_2^+. The major ions are considered to be maintained by scattered solar radiation (Ogawa and Tohmatsu, 1966; Keneshea et al., 1970; and Fujitaka et al., 1971) and the question as to whether scattered ultraviolet radiation can also account for the observed O^+ and N^+ must be investigated.

The sources of scattered radiation, which have been proposed as ionizing radiations, include Lyman alpha for NO, Lyman beta for O_2, and the HeI and HeII radiations at 584A and 304A, which can ionize most atmospheric constituents. The Lyman alpha and beta radiations can only contribute to the ion distribution below 130 km (Aikin and Goldberg, 1973). The HeI and HeII radiations, having a peak ionization rate between 150 and 200 km, were measured on 18.99, launched 35 minutes after 18.98. Fluxes of 16R for 584A and 8R for 304A were obtained (Paresce et al., 1973a, b).

These values are larger than the 10R for 584A and 1R for 304A used in computations of the nighttime ionosphere, e.g., by Fujitaka et al., (1971).

The presence of O^+ and N^+ below 200 km cannot be explained solely by the scattered radiations discussed above. These radiations would account for at most, 30 O^+ ions/cm^3 at 180 km and a factor of ten less at 150 km for the zenith angle ($\chi = 165^o$) of 18.98. For O^+, either another source of ionization and/or a small rate coefficient for the charge exchange reaction involving O^+ and O_2^+ is required. A third source might be instrumental, i.e., the partial dissociation of NO^+ and O_2^+ in the 10V bias field, prior to sampling. The situation is similar for N^+. Mechanisms for the production of N^+ include direct photoionization, dissociative ionization of N_2 and charge exchange between N_2^+ and N (Rishbeth et al., 1972). At night the primary source is photoionization by scattered solar EUV. This source is directly dependent on the atomic nitrogen content in the lower thermosphere. Additional production of N^+ by charge exchange between N_2^+ and N would require that the 28^+ observed be identified as N_2^+ rather than Si^+.

During both measurements 28^+ was observed in quantity. This constituent is shown on both Figure 1 (non-metallic constituents) and Figure 2 (metallic constituents) because of probable and indistinguishable contributions from N_2^+ and Si^+. Typical values shown range between 10 and 50 ions/cm^3. If 28^+ is identified as N_2^+, then it is difficult to explain the nighttime maintenance of this ion. The ion should be lost by ion-neutral reactions involving O and O_2. The nighttime scattered helium radiations account for, at their maximum, between 0.1 and 0.5 ions/cm^3 sec. They provide no contribution below 150 km although 28^+ is observed below this height.

Alternate possibilities include additional sources of ionization or the identification of 28^+ as Si^+. If Si^+, this constituent would have the typically long lifetime of atomic ions and be subject to a drift-controlled height structure. This last alternative is particularly attractive since reference to Figure 2 shows that 28^+ tracks the other metal ion distributions such as Mg^+.

The enhanced radiation, previously discussed, does not appear to modify the NO^+ and O_2^+ densities significantly below 180 km. The observations also indicate that above this altitude the NO^+ and O_2^+ distributions become increasingly sensitive to the drift of atomic ions, especially O^+. Enhancement of O^+ between the two flights increases the O_2^+ concentration by nearly an order of magnitude but there is less than a factor of 2 increase of NO^+. The slopes of the O_2^+ and NO^+ distributions do not coincide for 18.97 but are essentially the same for 18.98.

Above 200 km NO^+ is produced by the reaction between O^+ and N_2 (rate $\equiv k_1$). Dissociative recombination of NO^+ with electrons (rate $\equiv \alpha_{D1}$) is the only loss process so that under equilibrium conditions

$$NO^+ = \frac{k_1[O^+][N_2]}{\alpha_{D1}N_e} \simeq \frac{k_1[N_2]}{\alpha_{D1}}$$

For the latter step, it is assumed that $O^+ \simeq N_e$. A scale height can be derived which is indicative of the atmospheric temperature at the time of the flight. The profile of 18.98 rather than 18.97 is best suited for such analysis since the approximation is more accurate for nearly steady state conditions. The 18.98 data also show less scatter. The high altitude slope

of the 18.98 NO^+ profile yields a scale height of 31.7 km. This is consistent with an exospheric temperature of 1200°K and a model from the U.S. Standard Atmosphere (1966 Supplement) for this temperature can be adopted. This value can be favorably compared to the predicted exospheric temperature of approximately 1100°K for the geophysical conditions at the time of the flight.

The production of O_2^+ above 200 km is controlled by the reaction $O^+ + O_2 \rightarrow O_2^+ + O$ (rate $\equiv k_2$). Unlike NO^+, where loss is due solely to dissociative recombination, O_2^+ has an additional loss process represented by the charge exchange between O_2^+ and NO (rate $\equiv k_3$) which also becomes a source of NO^+ below 200 km. One can write under equilibrium conditions

$$[O_2^+] = \frac{k_2[O^+][O_2]}{\alpha_{D2}N_e + k_3[NO]}$$

where α_{D2} is the dissociative recombination coefficient for O_2^+.

For 18.98, $\chi = 165°$, $O^+ \cong N_e$ and provided the second term in the denominator is negligible compared to the first above 240 km ([NO] be less than 10^{-3} $[N_2]$, where $k_3 = 6.3 \times 10^{-10}$ cm^3 sec^{-1}, Johnsen et al., 1970), an expression is derived which is similar to that for NO^+. The products $\frac{k_1}{\alpha_{D1}}[N_2]$ and $\frac{k_2}{\alpha_{D2}}[O_2]$ must have nearly equal values to explain the data which shows that $[NO^+] \cong [O_2^+]$. This condition is satisfied because of the maintenance of large values for N_e at night, and is unique to the equator where vertical drift effects are large.

Assuming that the neutral atmosphere composition of the 1200°K U.S. Standard Atmosphere is correct, a comparison can thus be made between the

ion rate coefficients required for the ionosphere and those measured in the laboratory. At 1200°K, $\alpha_{D1} = 2 \times 10^{-7}$ cm^3 sec^{-1} (Bardsley, 1968) and $\alpha_{D2} = 1 \times 10^{-7}$ cm^3 sec^{-1} (Mehr and Biondi, 1969). The temperature dependence of k_1 and k_2 have also been measured (McFarland et al., 1973). These authors approximate the rate coefficients by $k_1 = 8 \times 10^{-14}(T/300)^2$ and $k_2 = 2 \times 10^{-11}(T/300)^{-0.4}$. The application of the laboratory derived rate coefficients gives an $[N_2]/[O_2]$ ratio which is within a factor of two of the atmospheric model used here.

The above analysis is not applicable for the flight of 18.97, when the solar zenith angle $\chi = 112^o$. At that time there was an upward drift of O^+ and electrons in addition to a transition in the ionizing flux, so that time variations must be considered in any detailed explanation of this profile.

Figure 2 compares the measured distribution of metal ions 23^+, Na^+; 24^+, Mg^+; 28^+, Si^+ or N_2^+; 39^+, K^+; and 40^+, Ca^+; for the two rocket flights. Typical spectra for the low altitude metallic ion data from flight 18.98 can be found in Aikin and Goldberg (1973).

Since neither spectrometer swept above mass 42, high pass filter mode data were employed to deduce information concerning heavier constituents. Following a technique outlined in Goldberg and Aikin (1971), high pass filter mode data for two AMU ranges ($1 \rightarrow \infty$; $32 \rightarrow \infty$) were used to deduce the relative sensitivity in this mode to the spectral mode. The T_B profile thus obtained represents all masses above 31^+ and is shown to 130 km. In the metallic belt between 90 and 100 km T_B is thought to be primarily Fe^+ (56^+), and above this height is O_2^+ (32^+). This latter conclusion is based on the result that at higher altitudes the T_B profile resembles O_2^+ during both flights.

Comparison of the concentrated metallic ion peak heights at 1938 and 0108 LMT illustrates that these long-lived atomic ions exhibit a downward drift during the course of the night. However, the total content remains fixed in the presence of this drift. A detailed discussion of this problem can be found in Aikin and Goldberg (1973).

Above 200 km on both flights, the light metallic ions 23^+, 24^+ and 28^+ are observed in concentrations of $10/cm^3$. Heavier metallic constituents, represented by 39^+ and 40^+, are observed in much smaller quantities at altitudes above 100 km. The high altitude limits of the metal ion profiles on 18.98 are not real, but caused by the background masking effect previously discussed.

The presence of light metallic ions at high altitudes (> 200 km) has previously been reported from rocket data at midlatitudes (Goldberg and Blumle, 1970) and satellite data (Taylor, 1973). These data would tend to suggest that long lived metallic ions are subject to ionospheric transport processes, and eventually disperse to regions far from their point of origin.

The drift and electron density measurements have also yielded interesting results. The velocity profile obtained from Thumba by ionogram analysis exhibits many of the typical properties observed at Jicamarca, Peru (Balsley, 1973) using incoherent backscatter techniques. These are principally the post-sunset upward drift followed by a more sustained downward drift virtually ending by midnight.

Returning to Figure 1, we note a certain amount of structure present in the N_i profile above 260 km on the 18.98 data but absent on the 18.97 profile. Rocket 18.97 was fired prior to any appearance of spread F on the ionograms, whereas 18.98 launch time ionograms showed a weak range spread

F condition. Hence, the structure observed may be associated with this equatorial phenomenon and/or drift.

There are also oscillations in N_i present at lower altitudes during both flights. No explanation for this observation exists at present although they may possibly be associated with tidal motions or with an unknown nighttime source of ionization near the 140 km level.

CONCLUSIONS

Two ion composition altitude profiles, representative of the behavior of the nighttime equatorial ionosphere, are presented. Between 200 and 300 km the dominant ion is O^+. This ion exhibits a nearly constant density of 2×10^3 cm^{-3} for a zenith angle of 112°. The F region exhibits a downward drift during the course of the night resulting in an increase in the concentration of O^+ by as much as a factor of 10^3 near 300 km. The O_2^+ concentration is correspondingly enhanced by O^+ charge exchange processes. The ion NO^+ exhibits little enhancement, consistent with theory. The ion N^+ exhibits some increase above 200 km, also caused by the downward drift.

Below 200 km, N_e, $[O_2^+]$ and $[NO^+]$ remain nearly unchanged between flights. Since the O^+ and N^+ densities in this region deplete too slowly to be accounted for by currently accepted loss rates; other sources of nighttime ionization are required. The constituent 28^+, if identified as N_2^+, is similarly overabundant below 200 km, but can be accounted for if identified as Si^+.

Light metal ions (Na^+, Mg^+, and possibly Si^+) are observed to altitudes of 300 km. Heavier metallics, such as Ca^+ and K^+ are observed to 200 km but in reduced quantity. The metallic ions are apparently influenced by ionospheric transport processes, which at the equator result primarily in vertical drift.

ACKNOWLEDGEMENTS

The results reported here were successfully obtained through the competent efforts of the Chemosphere Branch technical staff. In particular, we thank Messrs. Donald Silbert, Robert Farmer and Denis Endres for the development and preparation of the spectrometer flight package. Messrs. Roy Hagemeyer and Giles Spaid were largely responsible for the radio wave CW propagation experiment. We are indebted to Mr. John Jackson for his assistance in the interpretation of the ionosonde and CW propagation electron density data, and for his detailed trajectory analysis. We also thank the Indian Launch Range (TERLS) and the Goddard Sounding Rocket Division teams for their excellent cooperation and support.

TABLE CAPTION

Spectrometer characteristics for the instruments aboard payloads 18.97 and 18.98.

TABLE I

CHARACTERISTIC	18.97	18.98
Entrance aperature diameter (mm)	0.74	0.74
Rod length (mm)	101.6	101.6
Rod diameter (mm)	4.8	4.8
Sampling interval (sec)	1.56	1.69
Sweep range (AMU)	1-42	1-41
Mass range for high pass filter mode, T_B (AMU)	> 31	> 31
Time/unit mass (sec/AMU)	.030	.034
RF frequency (MHz)	2.85	2.85
Aperture attraction potential (volts)	-10	-10

REFERENCES

Aikin, A. C. and L. J. Blumle, Rocket Measurements of the E Region Electron Concentration Distribution in the Vicinity of the Geomagnetic Equator, J. Geophys. Res., 73, 1617, 1968.

Aikin, A. C. and R. A. Goldberg, Metallic Ions in the Equatorial Ionosphere, J. Geophys. Res., 78, 734, 1973.

Balsley, B. B., Nighttime Electric Fields and Vertical Ionospheric Drifts Near the Magnetic Equator, J. Geophys. Res., 74, 1213, 1969.

Balsley, B. B., Electric Fields in the Equatorial Ionosphere: A Review of Techniques and Measurements, J. Atmos. Terr. Phys., 35, 1035, 1973.

Bardsley, J. N., The Theory of Dissociative Recombination, J. Phys., B1, 365, 1968.

Bauer, S. J. and J. E. Jackson, Rocket Measurements of the Upper Atmosphere by a Radio Propagation Technique, J. Brit. IRE, 23, 139, 1962.

Chandra, H. and R. G. Rastogi, Spread F at Magnetic Equatorial Station Thumba, Ann. Geophys., 28, 37, 1972.

Farley, D. T., Jr., Observations of the Equatorial Ionosphere Using Incoherent Backscatter, (p. 446), Electron Density Profiles in Ionosphere and Exosphere, ed. by Jon Frihagen, John Wiley and Sons Inc., New York, 1966.

Fujitaka, K., T. Ogawa and T. Tohmatsu, A Numerical Computation of the Ionization Redistribution Effect of the Wind in the Nighttime Ionosphere, J. Atmos. Terr. Phys., 33, 687, 1971.

Goldberg, R. A. and L. J. Blumle, Positive Ion Composition from a Rocket-Borne Mass Spectrometer, J. Geophys. Res., 75, 133, 1970.

Goldberg, R. A. and A. C. Aikin, Studies of Positive Ion Composition in the Equatorial D Region Ionosphere, J. Geophys. Res., 75, 8352, 1971.

Goldberg R. A., Rocket Observation of Soft Energetic Particles at the Magnetic Equator, EOS Trans. AGU, 54, 1973.

Heikkila, W. J., Soft Particle Fluxes Near the Equator, J. Geophys. Res., 76, 1076, 1971.

Hudgins, J. I. and J. R. Lease, Tone Range-Telemetry Tracking System for Support of Sounding Rocket Payloads, NASA Spec. Publ. 219, 1967.

Johnsen, R., H. L. Brown and M. A. Biondi, Ion-Molecule Reactions Involving N_2^+, N^+, O_2^+ and O^+ Ions from 300°K to ~ 1 ev, J. Chem. Phys., 52, 5080, 1970.

Keneshea T. J., R. S. Narcisi and W. Swider, Jr., Diurnal Model of the E Region, J. Geophys. Res., 75, 845, 1970.

McFarland, M., D. L. Albritton, F. C. Fehsenfeld, E. E. Ferguson and A. L. Schmeltekopf, A Flow-drift Technique for Ion Mobility and Ion Molecule Reaction Rate Constant Measurements. II The Positive Ion Reactions of N^+, O^+ and N_2^+ with O_2 and O^+ with N_2 from Thermal to ~ 2 eV, J. Chem. Phys.. 59, 6620, 1974.

Mehr, F. J. and M. A. Biondi, Electron Temperature Dependence of Recombination of O_2^+ and N_2^+ Ions with Electrons, Phys. Rev., 181, 264, 1969.

Ogawa, T., and T. Tohmatsu, Photoelectric Processes in the Upper Atmosphere. 2. The Hydrogen and Helium Ultraviolet Glow as an Origin of the Nighttime Ionosphere, Rept. Ionosphere Space Res. Japan, 20, 395, 1966.

Paresce, F., S. Boyer and S. Kumar, Observations of the He II 304A Radiation in the Night Sky, J. Geophys. Res., 78, 71, 1973a.

Paresce, F., S. Boyer and S. Kumar, Evidence for an Interstellar or Interplanetary Source of Diffuse HeI 584A Radiation, to be published Astrophys. J. Letters, 1973b.

Rishbeth, H., P. Bauer, and W. B. Hanson, Molecular Ions in the F2 Layer, Planet. Space Sci., 20, 1287, 1972.

Seddon, J. C., Propagation Measurements in the Ionosphere with the Aid of Rockets, J. Geophys. Res., 58, 323, 1953.

Stassinopoulos, E. G. and Gilbert D. Mead, ALLMAG, GDALMG, LINTRA: Computer Programs for Geomagnetic Field and Field Line Calculations, NSSDA 72-12, National Space Data Center, Greenbelt, Maryland, February, 1972.

Taylor, H. A., Jr., Parametric Description of Thermospheric Ion Composition Results, J. Geophys. Res., 78, 315, 1973.

U. S. Standard Atmosphere Supplements, U. S. Government Printing Office, 1966.

FIGURES

Figure 1. Observed distribution of positive, non-metallic ion species in the nighttime E and F regions over Thumba: (left) upleg of rocket flight 18.97 at 1938 LMT, $\chi = 112^{\circ}$; (right) upleg of rocket flight 18.98 at 0108 LMT, $\chi = 165^{\circ}$.

Figure 2. Observed distribution of positive metallic ion species in the nighttime E and F regions over Thumba: (left) 18.97; (right) 18.98.

Figure 3. (upper) F-region electron density isopleths as a function of time for the night of March 9-10, 1970. (lower) Vertical drift velocity as a function of time.

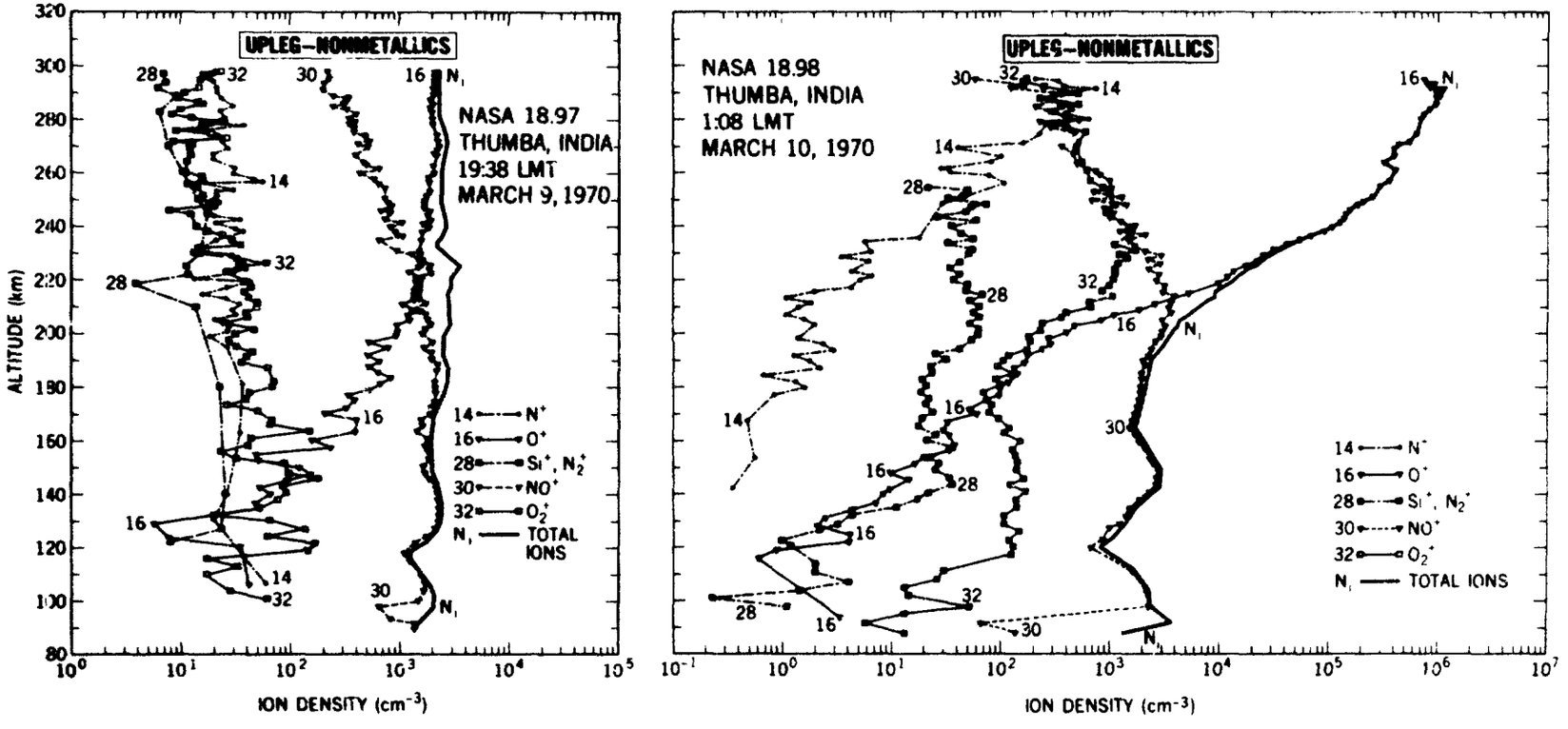
UPLEG–NONMETALLICS
NASA 18.97
THUMBA, INDIA
19:38 LMT
MARCH 9, 1970
14 N+
16 O+
28 Si+, N2+
30 NO+
32 O2+
Ni TOTAL IONS
ALTITUDE (km)
ION DENSITY (cm-3)
UPLEG–NONMETALLICS
NASA 18.98
THUMBA, INDIA
1:08 LMT
MARCH 10, 1970
14 N+
16 O+
28 Si+, N2+
30 NO+
32 O2+
Ni TOTAL IONS
ION DENSITY (cm-3)

Figure 1

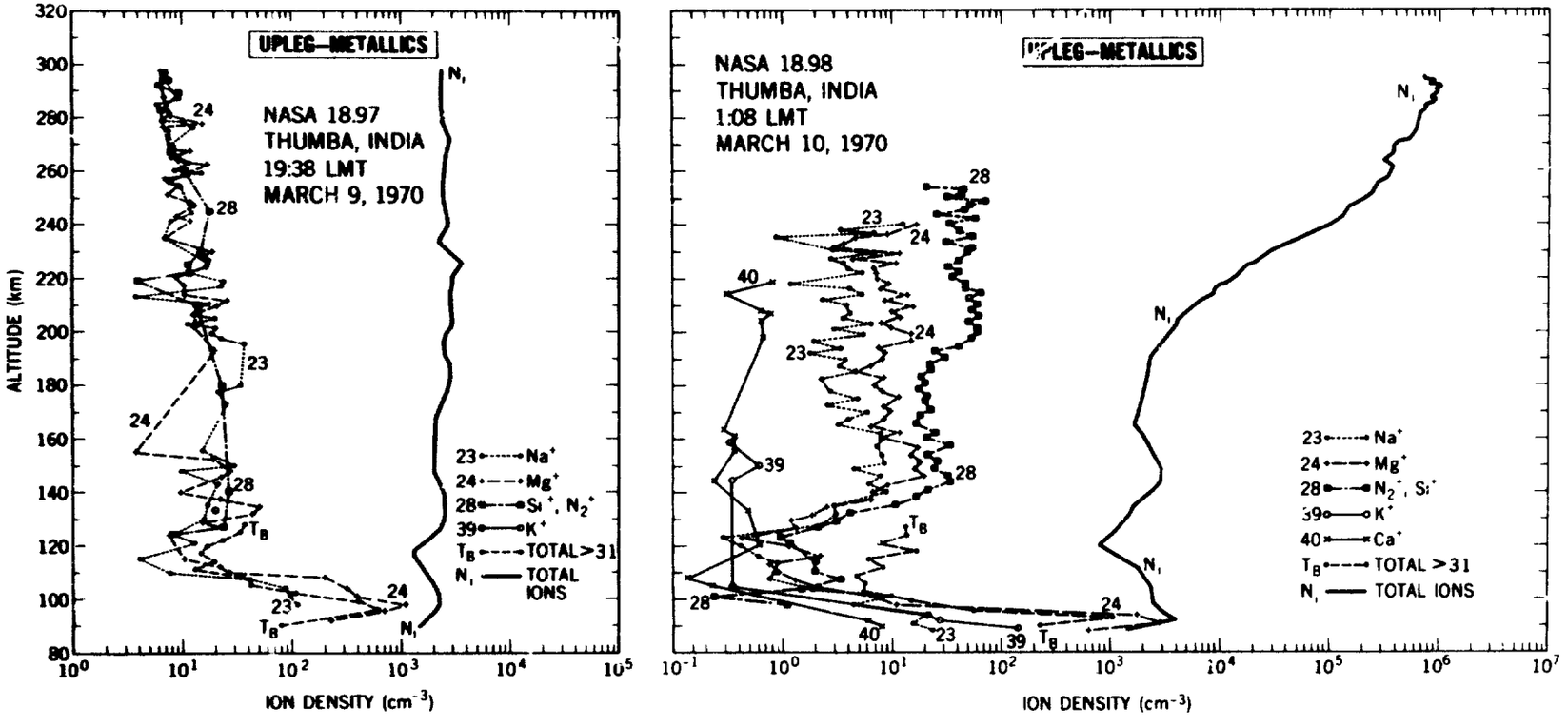
UPLEG–METALLICS
NASA 18.97
THUMBA, INDIA
19:38 LMT
MARCH 9, 1970
ALTITUDE (km)
ION DENSITY (cm⁻³)
23 Na⁺
24 Mg⁺
28 Si⁺, N₂⁺
39 K⁺
T_B TOTAL>31
N_i TOTAL IONS
UPLEG–METALLICS
NASA 18.98
THUMBA, INDIA
1:08 LMT
MARCH 10, 1970
ION DENSITY (cm⁻³)
23 Na⁺
24 Mg⁺
28 N₂⁺, Si⁺
39 K⁺
40 Ca⁺
T_B TOTAL >31
N_i TOTAL IONS

Figure 2

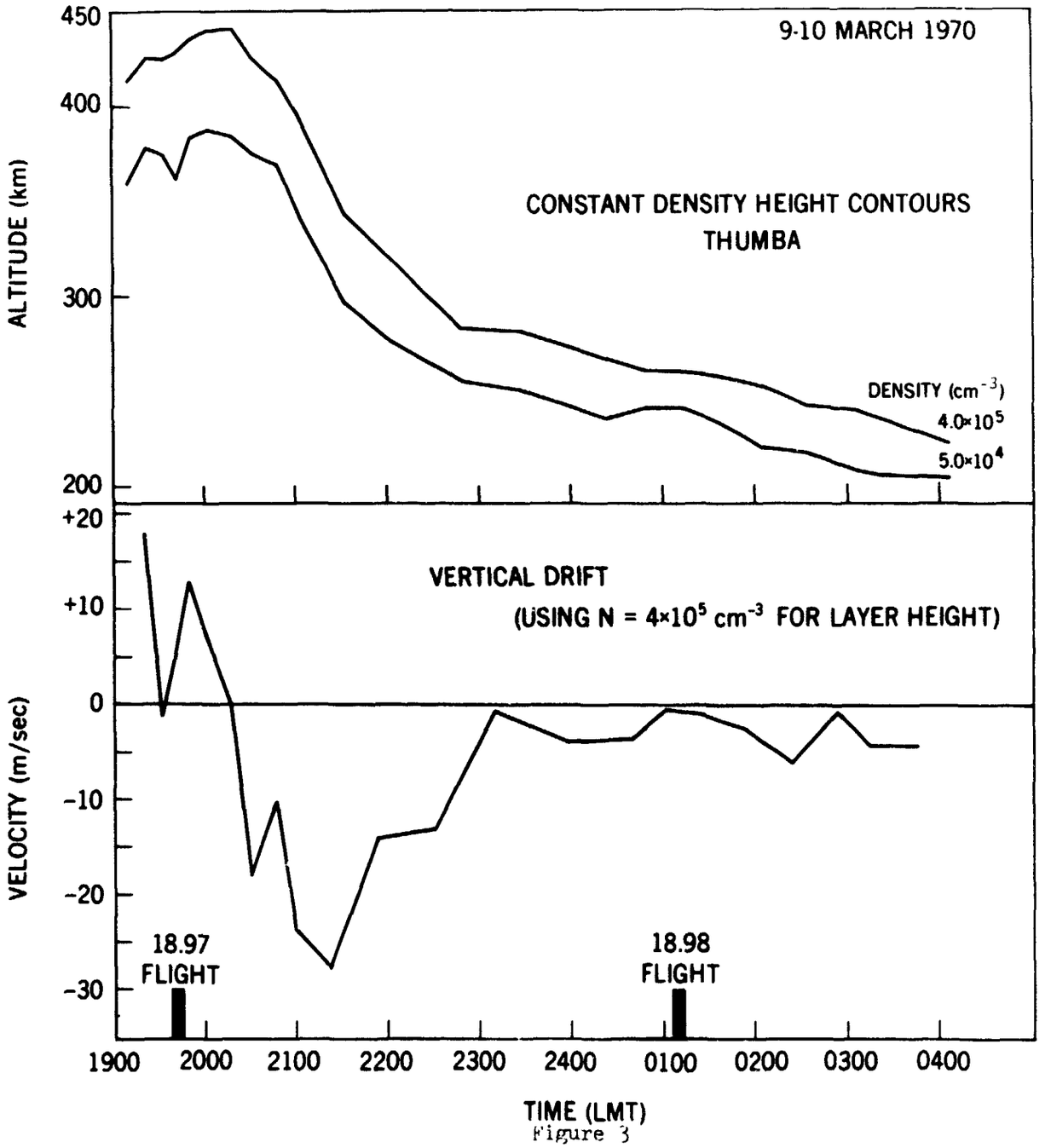
9-10 MARCH 1970
CONSTANT DENSITY HEIGHT CONTOURS
THUMBA
DENSITY (cm⁻³)
4.0×10⁵
5.0×10⁴
ALTITUDE (km)
450
400
300
200
VERTICAL DRIFT
(USING N = 4×10⁵ cm⁻³ FOR LAYER HEIGHT)
VELOCITY (m/sec)
+20
+10
0
-10
-20
-30
18.97
FLIGHT
18.98
FLIGHT
1900
2000
2100
2200
2300
2400
0100
0200
0300
0400
TIME (LMT)

Figure 3